Limnol. Oceanogr., 55(3), 2010, 1172–1187

doi:10.4319/lo.2010.55.3.1172

Temporal and spatial variability in the cycling of nitrogen within a constructed wetland: A whole-system stable-isotope-addition experiment

Dirk V. Erler,[a,*] Bradley D. Eyre,[a] and Leigh Davison[b]

[a] Centre for Coastal Biogeochemistry, School of Environmental Science and Management, Southern Cross University, Lismore, New South Wales, Australia

[b] Centre for Ecotechnology, School of Environmental Science and Management, Southern Cross University, Lismore, New South Wales, Australia

Abstract

Constructed wetlands attenuate effluent nutrients, are hydrodynamically well defined, and are a useful proxy for the study of nitrogen (N) transformation in eutrophic natural systems. A whole-system stable-isotope addition was undertaken to describe the N cycling within a constructed wetland. Addition of $^{15}NH_4^+$ and particulate organic ^{15}N ($PO^{15}N$) and a conservative tracer (Li^+) revealed that, initially, sedimentation of $PO^{15}N$ and assimilatory uptake of $^{15}NH_4^+$ near the wetland inlet removed most of the added ^{15}N. Denitrification of NO_3^- dominated inorganic N dynamics and was higher upstream than downstream owing to the greater availability of NO_3^- upstream. More NH_4^+ was mineralized upstream where PON settlement was highest, and settled PON started being mineralized within 14 d. Nitrification was insignificant upstream but was an important process in the downstream region of the wetland in spite of low oxygen concentration. In the medium term (2–8 weeks), the $PO^{15}N$ initially removed to the sediments continued to be mineralized, releasing $^{15}NH_4^+$ back to the water column. Remineralized ^{15}N spiraled through sediment and then macrophyte pools. A dry-out period resulted in a minor washout of N during the subsequent inundation. After 157 d, 30.8% ± 7.3% of the added ^{15}N was still in sediments, 7.4% ± 3.8% was in plants, 40.8% ± 8.3% had been lost most likely as $^{15}N_2$, and the remainder had been released in the wetland outlet water. Internal recycling retards the flow of N through wetlands, and short-term retention leads to eventual enhanced removal through denitrification.

Sewage treatment plant (STP) discharge can lead to persistent eutrophication and a loss in recreational and commercial value of receiving waterways (Cloern 2001). Constructed wetlands (CWs) are becoming increasingly popular as a tertiary treatment option for STPs. Constructed wetlands are known to remove nutrients from an effluent stream; however, the magnitude of this removal and the processes involved can vary over different timescales (Kadlec and Knight 1996; Vymazal 2007). The type and magnitude of nutrient-cycling processes may also vary spatially within wetlands (Johansson et al. 2004; Scott et al. 2005, 2008). Furthermore, disturbances to the wetland, including periodic dry out conducted as part of routine management protocols, are suspected of having important effects on N dynamics (Davidsson et al. 1997; Davidsson and Stahl 2000). However, the role of periodic dry out on wetland N cycling remains unclear (Ishida et al. 2006). In order to improve the management of CWs, it is critical to understand: (1) the temporal variability in the cycling of N during treatment, from the very short term (days) to the longer term (up to 6 months), (2) the spatial variability in N cycling, and (3) the ways in which N dynamics change in response to disturbances such as periodic dry out.

The fate of N within wetlands has been successfully studied using intact core incubations and mesocosm-scale experiments (Davidsson and Stahl 2000; Kadlec et al. 2005; Erler et al. 2008). These small- and medium-sized experiments have provided information on the type and rate of processes within constructed wetlands (Davidsson et al. 1997; Davidsson and Stahl 2000). Core and mesocosms can also be experimentally manipulated to study how process rates react under variable conditions such as season or site. We now understand that nutrients spiral through wetland systems and undergo a range of transformations along their route from inlet to outlet (Kadlec et al. 2005). These transformations include settlement and burial of particulate material, plant uptake of inorganic nutrients, volatilization and sorption, ammonification, nitrification, denitrification, and anammox (Kadlec et al. 2005; Vymazal 2007; Erler et al. 2008). The mechanisms by which NO_3^- can be removed from CWs include organotrophic and chemolithotrophic denitrification (including sulfide oxidation and dissimalatory nitrate reduction to ammonia [DNRA] [Burgin and Hamilton 2008], iron oxidation [Shrestha et al. 2009], and anammox [Erler et al. 2008]). One of the main drawbacks of core and mesocosm experiments, however, is that they are logistically difficult to maintain beyond the medium term (1–2 months). Furthermore, the outcomes from core and mesocosm studies need to be validated in full-scale systems. Achieving this validation in full-scale systems, however, poses some methodological challenges.

The study of full-scale wetlands is often achieved with mass-balance models (Cameron et al. 2003). Mass-balance models provide good information on net nutrient removal but are less useful at tracing the fate of N within a wetland. A range of stable-isotope techniques can be employed to elucidate N removal processes. The simplest of these is the use of natural abundance stable-isotope ratios to estimate

* Corresponding author: dirk.erler@scu.edu.au

the fate of, and to quantify the cycling rates of, N in wetlands (Lund et al. 1999; Reinhardt et al. 2006). This technique can be very useful but relies on the existence of natural variability in the isotope signatures of the different N pools. This natural variability can often be subtle and difficult to quantify accurately.

Whole-system stable-isotope-addition experiments can greatly augment information from traditional mass-balance and natural abundance studies. The whole-system approach is essentially a dosing experiment where stable isotope is added and then traced through an ecosystem. The technique can be used to estimate the storage and release of nutrient between dominant pools and to calculate the rates of nutrient cycling within the studied ecosystem (Tobias et al. 2003*a*; Gribsholt et al. 2005). Furthermore, complementary information on sediment fluxes can be determined by conducting small-scale core incubations during the whole-system stable-isotope addition (Tobias et al. 2003*b*). Despite its advantages, the whole-system stable-isotope-addition technique, to our knowledge, has never been applied to trace the fate of N in a full-scale surface-flow wetland.

The objective of this study was to use whole-system stable-isotope additions to describe N cycling within a full-scale surface-flow wetland over a range of timescales (very short term [1–2 d], short term [1–2 weeks], medium term [2–8 weeks], and long term [≈ 6 months]), along the wetland flow gradient and during a dry-out disturbance. We hypothesize that: (1) the flow of N through the studied wetland will be retarded through settlement of particulate organic nitrogen (PON), and this will facilitate spiraling of N and eventually lead to enhanced loss through denitrification; (2) the wetland will be spatially variable, and dissolved oxygen will regulate the type and extent of N cycling processes; and (3) a dry-out disturbance will facilitate nitrification and denitrification processes, enhancing N removal. Owing to the lack of groundwater exchange and the well-defined inlet and outlet points, constructed wetlands are a much more tractable system to study N cycling than natural wetlands, ponds, and impounded streams and rivers. The study of N cycling in constructed wetlands therefore can help us to understand N cycling in natural systems that are affected by eutrophication or fluctuations in water level.

Methods

Study site—The trial was conducted at a 9-yr-old surface-flow CW used to tertiary treat effluent from a 3 megaliter (ML) d^{-1} STP located in Casino, New South Wales, Australia (Fig. 1). The constructed wetland consisted of three parallel wetlands labeled A, B, and C (13,500, 8441, and 2686 m^2, respectively) with an average water depth of 0.1 m. Three macrophytes dominated the wetland, *Typha orientalis*, *Bulboschoenus medianus*, and *Phragmites australis*, which accounted for 62%, 35%, and 3% of the wetland plant dry weight, respectively. The distribution of the macrophytes within the wetland is shown in Fig. 1. The wetland received on average about 2.5 ML d^{-1} of water from the STP's 4-km^2 effluent storage

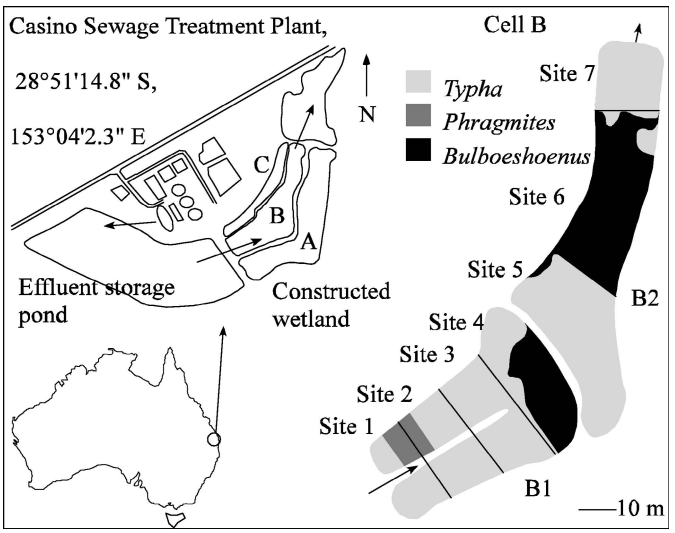

Fig. 1. The Casino constructed wetland study site showing the wetland cell (cell B), the subcells (B1 and B2), and the sampling sites (1–7) used for the whole-system stable-isotope-addition experiment. The distribution of the three dominant vegetation types is also shown.

pond. This storage pond maintained a consistent bloom of phytoplankton (mainly *Microcystis aureginosa*) throughout the study period. Each individual wetland cell could be flooded separately, and under normal operating conditions, each cell would receive flows of between 0.5 and 1.5 ML d^{-1} for 3–4 weeks (inundation phase). The wetland cells were then dried for 1–2 weeks (dry-out phase) prior to the next inundation phase.

Cell B was chosen for the whole-system trial because of its manageable size. The cell consists of two subcells (B1 and B2 of 4151 and 4290 m^{-2}, respectively) joined by four 300-mm-diameter drain pipes. These drains are referred to as the middle drains (MDs). At the wetland inlet, two inline Flanged Woltmann–type flow meters (DANE IRT) were installed in each of the inlet pipes. These recorded cumulative flow into the CW. A StarFlow Ultrasonic Doppler flow meter (Unidata) was placed in each of the two wetland outlet drain pipes. These measured and logged water flow and temperature every 10 min. Seven sites (1–7) were identified within cell B from inlet to outlet (*see* Fig. 1). Within each site, several sampling locations (up to 4) were assigned in order to ensure that we accounted for spatial variability within sites.

Tracer delivery—We attempted to label the most abundant N pool in the wetland inlet water, i.e., particulate organic nitrogen (PON), because we expected it to be an important regulator of wetland dynamics. In order to label the PON pool, we incubated wetland inlet water with $^{15}NH_4^+$, since it can be assimilated easier than NO_3^-. Enrichment of the PON pool was achieved by enriching 2700 liters of storage pond water in a fiberglass tank with $^{15}NH_4Cl$ (0.49 mol ^{15}N) for 3 h (06:00 to 09:00 h on the 16 October 2007). The conservative tracer LiCl (22.4 mol Li^+) was also dissolved in the enrichment tank. To determine the

NH_4^+ concentration and enrichment time required to maximize uptake of $^{15}NH_4^+$ into PON, and minimize the production of labeled dissolved organic ^{15}N ($DO^{15}N$) and $^{15}NO_3^-$, a bottle incubation trial was conducted prior to the whole-system tracer release. The bottle incubations involved the addition of three different concentrations of $^{15}NH_4^+$ (0.07, 0.17, and 0.35 mmol L^{-1}) to 1-liter Schott bottles containing storage pond water. Three bottles were used for each concentration, and three additional bottles without $^{15}NH_4^+$ amendment were used as controls. The bottles were suspended off a walkway into the surface water of the effluent storage pond. At 0, 1, 2, 3, and 4 h intervals (06:00 h to 22:00 h), the concentration and isotope ratios of $PO^{15}N$, $^{15}NH_4^+$, $^{15}NO_3^-$, and $DO^{15}N$ in the bottles were determined (*see* below). The results showed that the optimum enrichment time and $^{15}NH_4^+$ concentration were 3 h and 0.17 mmol L^{-1}, respectively (data not shown). The enriched tank water was then gravity fed into the inlet pipes of cell B over a 1-h period. This tank water can be thought of as an enriched plume. The entire enrichment procedure, except for the LiCl addition, was repeated the following day (17 October 2007). The concentration and isotope signatures of PON, NH_4^+, NO_3^-, and dissolved organic nitrogen (DON) were measured before, and twice during, the enrichment period (*see* Water sample collection and analysis section).

Water flow into cell B was turned on and set at between 0.8 and 1.2 ML d^{-1}, the normal operating range, 1 week prior to the whole-system stable-isotope-addition trial. The inundation phase continued until the 31 October 2007 (day 14 after tracer release), at which time flow was turned off. The dry-out phase lasted until the 11 November 2007 (day 25 after tracer release). Sediments in the wetland remained moist but not saturated by the end of the dry-out phase. Flow resumed into cell B, and this inundation phase lasted $\approx$ 4 weeks (ended on day 54, 10 December 2007).

Water sample collection and analysis—For the long-term nutrient monitoring (6 March to the 24 September 2007), water samples were collected during inundation periods twice weekly from the wetland inlet and outlet. Water samples ($\approx$ 500 mL) were collected in acid-rinsed high-density polyethylene (HDPE) bottles. Immediately after collection, subsamples (10 mL each) were filtered (0.45-μm syringe filter, Sartorius) for dissolved inorganic N (DIN) and total dissolved N (TDN) into 12-mL polypropylene and polycarbonate sample tubes, respectively. A further 10 mL of unfiltered sample were collected for total N (TN) analysis in a 12-mL polycarbonate sample tube. Water-quality data (O_2, pH, conductivity) were logged every hour at the CW inlet and outlet with DataSonde® 3 probes.

During the whole-system trial, water samples for N concentration and isotope signature analysis were collected from the incubation tanks before, and twice during, the tracer enrichment. Samples were also collected from the wetland inlet, the MDs, and the wetland outlet every 4 h for 3 d starting at the beginning of the tank enrichments. Sampling was then conducted twice a day ($\approx$ 07:00 and 16:00 h) for 14 d. Water samples were not collected between days 14 to 25 because the wetland flow was off. Twice-daily sampling was conducted between days 26 to day 33. Daily sampling was then carried out for a further week, and weekly sampling was conducted after that until the wetland was next turned off (day 54). Water sampling ceased after this time.

Sampling involved collection of approximately 500 mL of water in an acid-rinsed HDPE sample bottle. Within 10 min after collection, an aliquot of the sample was sucked into a clean 60-mL syringe and passed through a 25-mm Teflon syringe filter manifold containing a 25-mm Glass fiber (GF) F filter paper (Whatman) to trap $PO^{15}N$. A 12-mL aliquot of this filtrate was collected into an exetainer vial (Labco) containing 50 μL of 2 mol L^{-1} NaOH for dissolved gaseous ^{15}N analysis (sealed without headspace). A tube was attached to the filter manifold so filtrate could be added to the bottom of the exetainer and bubbles could be avoided. Ten milliliters of deionized water were passed through the filter paper before it was removed, wrapped in aluminum foil, and stored frozen. The filtered volume was dependent on the turbidity of the sample; for the inlet samples, this was generally around 10 mL, and for the MDs and the outlet samples, around 50 mL was filtered. A 10-mL unfiltered aliquot was collected for TN analysis from the remaining sample, and the rest was filtered through a 25 mm diameter GF-75 (Whatman) filter paper in a 500-mL Millipore vacuum-filtration manifold. The filtrate was split as follows: two 100-mL samples into 125-mL HDPE bottles for $^{15}NH_4^+$ and $^{15}NO_3^-$ (including $^{15}NO_2^-$) analysis; a 100-mL sample into a 125-mL HDPE bottle containing 500 μL of $ZnCl_2$ for $DO^{15}N$ analysis; and two 10-mL samples into 12-mL tubes for DIN and DON analysis.

The $^{15}NH_4^+$ and $^{15}NO_3^-$ in filtered-water samples were collected on acidified GF-D (Whatman) filter papers via the acid trap diffusion protocols described by Holmes et al. (1998) and Sigman et al. (1997). The amount of $^{15}NH_4^+$ and $^{15}NO_3^-$ trapped on the filter papers was determined by isotope ratio mass spectrometry (IRMS, Thermo Delta V Plus IRMS) after combustion on an elemental analyzer (Thermo Flash EA 1112). Both $^{15}NH_4^+$ and $^{15}NO_x^-$ control samples were also analyzed via the diffusion protocol. All EA-IRMS samples were standardized against the ultrapure calibration standards $(NH_4)_2SO_4$ (52‰). For $PO^{15}N$ analysis, stored filters were first freeze-dried before being packed into tin capsules for analysis via EA-IRMS. For $DO^{15}N$ analysis, NaS_2O_8 (5.2 g) was first added to a 100-mL water sample and autoclaved (120°C for 30 min) to convert DON to NO_3^-. Devarda's alloy (300 mg) was added to convert NO_3^- to NH_4^+, and enough NaOH (2 mol L^{-1}) was added to raise the pH (> 10) in order to convert NH_4^+ to NH_3. A 10-mL GF-D filter paper containing 5 mol L^{-1} H_2SO_4, sandwiched between two Teflon filter papers, was added to trap the NH_3. Filter papers were subsequently analyzed for $^{15}NH_4^+$. A simple three-member mixing model (Fry 2005) was used to isolate the $DO^{15}N$ signature from the mixture of $DO^{15}N$, $^{15}NH_4^+$, and $^{15}NO_x^-$. Several ^{15}N urea controls were also analyzed to determine the accuracy of this $DO^{15}N$ method (*see* Results), and each $DO^{15}N$ sample was analyzed in duplicate.

The ^{15}N content of dissolved nitrogenous gas was determined following the addition of a He headspace to the 12-mL dissolved gas sample vials. Nitrogenous gases, including $^{15}N_2$ and $^{15}N_2O$ (i.e., ^{14}N-^{15}N, ^{15}N-^{15}N, ^{14}N-^{15}N-O, and ^{15}N-^{15}N-O), were not separated and were analyzed together; they are collectively referred to as $^{15}N_2$ for the remainder of this paper. The $^{15}N_2$ concentrations were determined via gas chromatography coupled to IRMS, where the gas chromatograph (Thermo Trace Ultra GC) was interfaced (Thermo Finnigan GC Combustion III) to the isotope ratio mass spectrometer calibrated against pure tank N_2 standards. Values are reported with respect to N_2 in air. Aliquots of atmospheric air were analyzed prior to samples each day to test for accuracy and precision. All nutrient samples were analyzed colormetrically by flow-injection analysis (Eyre and Ferguson 2005). The concentration of the conservative Li^+ tracer was determined by inductively coupled plasma optical emission spectroscopy (ICP-OES) using a Perkin Elmer dual view PV4300.

Sediment and macrophytes—The mass and isotope signature of N stored in the sediments and macrophyte pools were determined in the wetland (sites 1–7 in Fig. 1) 1 month prior to tracer addition to calculate background isotope abundance. Sediments were also sampled 2, 8, 15, 30, 42, and 157 d after the tracer addition. Macrophytes were also sampled before and 2, 9, 15, 32, 43, and 157 d after tracer addition. Sediments were collected at each sampling site, at each location, as follows: first, non-submerged dead plant material was carefully removed from an area roughly 30 × 30 cm. A Perspex core, 9.0 × 50 cm, was placed over the sediment surface, and a knife was used to cut around the surface detritus. The core was then pushed into the sediment (≈ 30 cm), stoppered, and removed. The surface water from the cores was decanted through a 0.5-mm strainer and the trapped particulates were returned to the core. The core contents were carefully compacted and then extruded. The sediment core was split into three depth subsamples, 0–2.5 cm, 2.5–5 cm, and 5–10 cm. Sediments were placed into sampling bags and iced. Two cores were collected from each sampling location within each site.

For the macrophyte sampling, two individuals of each type of macrophyte at each sampling location were selected and carefully pulled from the sediment using a shovel. Care was taken to remove as much root material as possible. The plants were washed with tap water to remove sediments from around the roots, cut into pieces, and placed into plastic bags for transport. At each sampling location, the total coverage and distribution of macrophytes were also estimated by counting the number of individual plants in four 50 × 50 cm quadrats roughly 5 m apart.

Sediment samples were stored for up to 4 months before processing. For processing, thawed sediments were first weighed and then thoroughly homogenized. A 10-g portion was then weighed into a 50-mL centrifuge tube together with 40 mL of 2 mol L^{-1} KCl. The sediment slurry was shaken for 1 h and then centrifuged. The supernatant containing pore water and easily desorbed NH_4^+ was decanted into a syringe, and 10 mL were filtered (0.45-μm Minisart, Sartorius) into vials for DIN analysis. The remaining 30 mL were collected into an acid-rinsed 100-mL HDPE bottle for $^{15}NH_4^+$ analysis. The sediment samples were twice rinsed with Milli-Q water (40 mL) before being freeze dried. Dried sediments were ground and weighed out for analysis via EA-IRMS. The $^{15}NH_4^+$ content of the KCl extract was determined as described earlier.

On return to the laboratory, macrophyte material was firstly weighed and then oven dried (70°C) to constant weight. All plant samples were milled and then ground to a fine powder in a ball mill. Subsamples of ground material were weighed and analyzed via EA-IRMS.

Core incubations—Three separate core incubations were performed during the whole-system isotope-addition trial: one just prior to the end of the CW inundation phase (day 10 after tracer release), one during the dry-out phase (day 22), and one a week after the start of the second inundation phase during the whole-system trial (day 33). For the core incubations, two cores were collected at each site along the wetland flow path using 9.0 × 50 cm (interior diameter × height) Perspex cores as described already. The cores were transported back to the laboratory, where they were placed in an incubation tank at 22°C. Filtered wetland water (0.45 μm) from the middle drains (dissolved oxygen [DO] of 0.17 mmol L^{-1}), for cores from sites 1 to 4, and from the wetland outlet (DO of 0.1 mmol L^{-1}), for sites 5 to 7, was added to completely fill each core (≈ 500 mL). For the dry-out phase incubation, water was collected from the outlet of cell A (DO of 0.1 mmol L^{-1}). Magnetic stirrer bars, slowly turned with a large external rotating magnet, were placed into each core. Two 500-mL clear glass bottles were also filled with filtered wetland water, as controls, and placed in the incubation tanks. The cores were sealed and left to incubate in the dark.

Soon after the cores were sealed, a sample of the wetland water from the incubation tanks was collected for $^{15}NH_4^+$, $^{15}NO_3^-$, $^{15}N_2$, and nutrient analysis as already described. After 2 h, one of each core from each of the sampling sites was opened, and a sample was collected for isotopic and nutrient analysis. After another 2 h, the second of the cores was opened and sampled. The sampling time was kept short to ensure the cores did not become anoxic. Samples were processed as described earlier.

Calculations—To estimate the very short-term rates of DIN cycling, an isotope mass balance was constructed between the time of stable-isotope release and the point of maximum concentrations of Li^+ at the MDs and the outlet (i.e., the Li^+ breakthrough points). The mass balance assumes that stable-isotope tracer was added as a plume of enriched water into the wetland (Fig. 2) and was diluted by the surrounding wetland water as it moved along the flow path. At the MDs and the outlet, the size of the diluted plume was calculated to determine the rates of DIN cycling. For ease of calculation, it was assumed that evapotranspiration (ET) was negligible. Other studies of this wetland (D. V. Erler unpubl. data) have shown that ET can be significant in the summer months; however, rates of

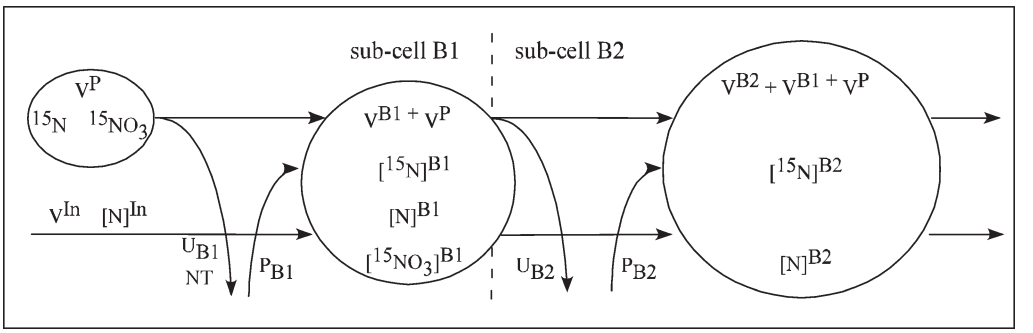

Fig. 2. Conceptual diagram of the movement and dilution of the ^{15}N tracer plume through the wetland used to develop the short-term N cycling rate equations. The variables in the figure are described in Table 1.

ET were generally lower during the time of the experiment ($\approx$ 2% of inlet water lost to ET). All calculations and variable descriptions are detailed in Table 1.

An inventory of ^{15}N was made to assess the movement of ^{15}N within the wetland over time. The amount of ^{15}N moving through the wetland as $PO^{15}N$, $^{15}NH_4^+$, $^{15}NO_3^-$, and $DO^{15}N$ was calculated by multiplying the excess ^{15}N concentration of each parameter by discharge volume. The excess ^{15}N concentration is the Δatom % ^{15}N (i.e., the atom % ^{15}N of a particular pool after tracer addition minus the atom % ^{15}N of that pool prior to tracer addition) multiplied by the concentration of the N parameter.

For sediments and macrophytes, the inventory was calculated for days 2, 6, 9, 15, 30, 45, and 157. Macrophytes were often sampled the day after sediments, and the inventory is given for the sediment sampling days. The excess ^{15}N in the sediments from different sampling sites was calculated by multiplying the Δatom % ^{15}N of the sediment (i.e., atom % ^{15}N of a particular pool after tracer addition minus the atom % ^{15}N of that pool prior to tracer

Table 1. Equations and variables used for the very short-term N cycling rates. The conceptual diagram used to develop these equations is shown in Fig. 2.

1 $$\%\Delta^{15}N_{B1} = \frac{^{15}N - [^{15}N]^{B1} \times (V^{B1} + V^P)}{^{15}N}$$

2 $$\%\Delta^{15}N_{B2} = \frac{[^{15}N]^{B1} \times (V^{B1} + V^P) - \left([^{15}N]^{B2} \times V^{B2}\right)}{[^{15}N]^{B1} \times (V^{B1} + V^P)}$$

3 $$U_{B1} = \frac{\%\Delta^{15}N_{B1} \cdot [N]^{In} \cdot V^{In}}{t_1 \cdot A_1}$$

4* $$U_{B2} = \frac{\%\Delta^{15}N_{B2} \cdot [N]^{B1} \cdot V^{In}}{t_2 \cdot A_2}$$

5 $$P_{B1} = \frac{[N]^{B1} \cdot (V^{B1} + V^P) - (^{15}N + V^P \cdot [N]^{In}) \cdot (1 - \%\Delta^{15}N_{B1}) - \frac{[N]^{In} + [N]^{B1}}{2} \cdot V^{B1}}{V^{B1} + V^P}$$

6 $$P_{B2} = \frac{[N]^{B2} \cdot (V^{B2} + V^{B1} + V^P) - (V^{B1} + V^P) \cdot [N]^{B1} \cdot (1 - \%\Delta^{15}N_{B2}) - \frac{[N]^{B1} + [N]^{B2}}{2} \cdot V^{B2}}{V^{B2} + V^{B1} + V^P}$$

7 $$M_{B1} = \frac{P_{B1} \cdot V^{In}}{t_1 \cdot A_1}$$

8 $$M_{B2} = \frac{P_{B2} \cdot V^{In}}{t_2 \cdot A_2}$$

9 $$NT = U_{B1} \times \frac{[^{15}NO_3]^{B1} \times (V^{B1} + V^P) - {}^{15}NO_3}{M^{15}N_{B1} - [^{15}N]_{B1} \cdot (V^{B1} + V^P)}$$

$\%\Delta^{15}N_{B1}$ and $\%\Delta^{15}N_{B2}$	Percent change in the quantity of $^{15}NH_4^+$ in the water during enriched plume transport between the inlet and the MDs ($_{B1}$) and the MDs and the outlet ($_{B2}$), respectively.
^{15}N and $^{15}NO_3$	Quantity of $^{15}NH_4^+$ and $^{15}NO_3^-$ in the enriched plume prior to release (mmol)
$[^{15}N]^{B1}$, $[^{15}N]^{B2}$, $[N]^{B1}$, $[N]^{B2}$, $[N]^{In}$, and $[^{15}NO_3]^{B1}$	Concentrations of $^{15}NH_4^+$ (^{15}N), NH_4^+ (N), or $^{15}NO_3^-$ ($^{15}NO_3$) at the MDs (^{B1}), the outlet (^{B2}), and entering the wetland (^{In}) (mmol L^{-1})
V^{B1}, V^{B2}, V^P, and V^{In}	Diluted volumes of the enriched plume at either the MDs or the outlet*, the volume of the enriched plume, and the volume entering the wetland in a given time t, respectively (L)
U_{B1} and U_{B2}	Uptake rates of NH_4^+ for subcells B1 and B2, respectively (mmol m^{-2} h^{-1})
t_1 and t_2	Time taken to reach the breakthrough point at the MDs and outlet, respectively (h)
A_1 and A_2	Surface area of subcells B1 and B2 (m^{-2})
P_{B1} and P_{B2}	Production rate of NH_4^+ in subcells B1 and B2† (mmol L^{-1})
M_{B1} and M_{B2}	Mineralization rate in subcells B1 and B2 (mmol m^{-2} h^{-1})
NT	Nitrification rate‡,§ (mmol m^{-2} h^{-1})

* For Eq. 4, it is assumed that V^{In} is equal to the volume leaving subcell B1, i.e., negligible evapotranspiration.
† The dilution volumes were calculated from the Li^+ concentration data and the equations of Tobias et al. (2001).
‡ The production of NO_3^- was estimated by substituting NO_3^- concentrations into Eqs. 5 and 6 and removing the parameters U_{B1} and U_{B2}.
§ For the purposes of the calculations, the uptake of NO_3^- into microbes or plants was assumed to be minor.

Table 2. Average concentration of N species (mmol L^{-1}), percent contribution to total N in wetland inlet and outlet, and percent removed between inlet and outlet (accounting for water loss through the wetland) over a 7-month monitoring period (Mar–Sep 2007).

	Average inlet concentration (mmol L^{-1}) and % of total inlet N		Average outlet concentration (mmol L^{-1}) and % of total outlet N		% removed through wetland
TN	0.560±0.015	100	0.160±0.005	100	70.4±0.8
NH_4^+	0.028±0.002	5.4±0.6	0.019±0.002	10.4±1.1	51±4.5
NO_3^-	0.133±0.007	23.6±1.0	0.046±0.003	27.8±1.4	64.3±1.9
PON	0.301±0.012	52.4±1.1	0.016±0.003	9.8±1.4	93.4±1.0
DON	0.099±0.008	18.7±1.3	0.080±0.004	51.9±1	23.0±24.3

addition) by the total N content per gram of sediment. Using a sediment weight–to–area conversion and the measured area of each sampling location, the excess ^{15}N per m^2 could be determined for each site in the CW. The pore-water excess $^{15}NH_4^+$ concentration in the KCl extracts was divided by the surface area of the cores, corrected for water content (i.e., porosity) of the sediments, and divided by the sediment sampling area to give a value in square meters. This was averaged between the sediment depths and multiplied by the area of each site.

For macrophytes, the amount of N in each plant species was multiplied by the number of shoots of that plant species in a sampling location. These values were multiplied by the Δatom % ^{15}N of the plant sections to determine the distribution of excess ^{15}N within the wetland. The missing ^{15}N at each time period was assumed to have been lost to the atmosphere. Note that this value reflects the cumulative error of all other estimates.

For the core incubations, rates of $^{15}N_2$ (i.e., ^{14}N-^{15}N and ^{15}N-^{15}N), $^{15}NH_4^+$, and $^{15}NO_3^-$ production were calculated as the linear increase in excess ^{15}N concentration during incubation. This was divided by core area to give a rate in nmol m^{-2} h^{-1}.

Statistical calculations—Reported mean concentrations of water-column parameters are accompanied by standard errors. Estimates of the sediment and macrophyte excess ^{15}N at each site are the means (± standard error) of all samples collected within that sampling site. For the macrophyte estimates, there is an additional error associated with the calculation of macrophyte coverage.

A repeated measures analysis of variance was performed to determine if the sediment and macrophyte ^{15}N content varied significantly over time. After testing for sphericity (Mauchly's test) we used the Huynh-Feldt test to determine the significance of within-subject variability (SPSS 17.0). For the mass-balance calculations, total errors were calculated as the square root of the sum of the individual errors each squared.

Results

Net N removal and transformation—Nitrogen was consistently removed in the wetland over the 7-month monitoring period (Table 2). Total N and PON in the wetland inlet water increased between June and September 2007 (Fig. 3A,B) as temperature and day-lengths became more favorable for phytoplankton growth in the effluent storage pond. Total N in the wetland outlet water often declined after the start and increased toward the end of an inundation period (Fig. 3A). The removal of PON was the dominant mechanism for removing TN from the inlet water (93.4% ± 1.0% removed). There was a 64% ± 2% removal of NO_3^- between inlet and outlet (Table 2). Average NH_4^+ concentrations decreased between the inlet and outlet (average percentage removal 51.1% ± 4.5%). Removal of DON was the lowest of all the N species. Flow rates varied from 0.5 to 2.2 ML d^{-1} and averaged 1.33 ± 0.03 ML d^{-1} over the monitoring period. For DON and NH_4^+, concentrations in the wetland outlet water tended to increase during an inundation period (Fig. 3D,E). Hydroperiod varied, but generally 3–4 weeks of inundation were followed by 1–2 weeks of dry-out (Fig. 3G). Oxygen concentrations averaged 321 ± 20 μmol L^{-1} in the wetland inlet and 59 ± 10 μmol L^{-1} in the wetland outlet.

Tracer addition experiment—The $\Delta\delta^{15}N$ (i.e., the $\delta^{15}N$ after tracer addition minus the $\delta^{15}N$ before tracer addition) of the inlet water-column parameters (NH_4^+, NO_3^-, PON, and DON) are shown in Table 3. There was significant enrichment of all $\delta^{15}N$ pools (Table 3). The NH_4^+ pool had the highest isotopic enrichment by far, but the excess ^{15}N concentrations of NH_4^+ and PON in water entering the wetland were similar (Table 3). The concentration of NH_4^+ in the inlet water was doubled by the addition of the label, but it was similar to the average NH_4^+ concentration in the wetland inlet water over the 7-month monitoring period (i.e., 3 μmol L^{-1}). Excess $^{15}N_2$ concentrations did not increase during enrichment.

The conservative tracer response curve in Fig. 4A and shows that peak concentrations of Li^+ at the MDs and the outlet occurred 8 and 16 h after the start of tracer release, respectively. Using the centroid of the two curves, the nominal hydraulic residence times were calculated to be 13 h between inlet and MDs and 26 h for the entire wetland.

The production of $^{15}N_2$ is shown in Fig. 4B, which shows minor peaks in excess $^{15}N_2$ concentrations in the water at the MDs and the outlet during the two enrichments. This is followed by a stable period, where excess $^{15}N_2$ concentrations remain below 10 nmol L^{-1}. Beginning on day 6, there is a spike in excess $^{15}N_2$ concentrations at both the MDs and the outlet lasting until day 9. Excess $^{15}N_2$ concentrations approached zero until the end of the inundation period. A small peak in excess $^{15}N_2$ concentration was observed in the outlet water at the start of the second inundation phase.

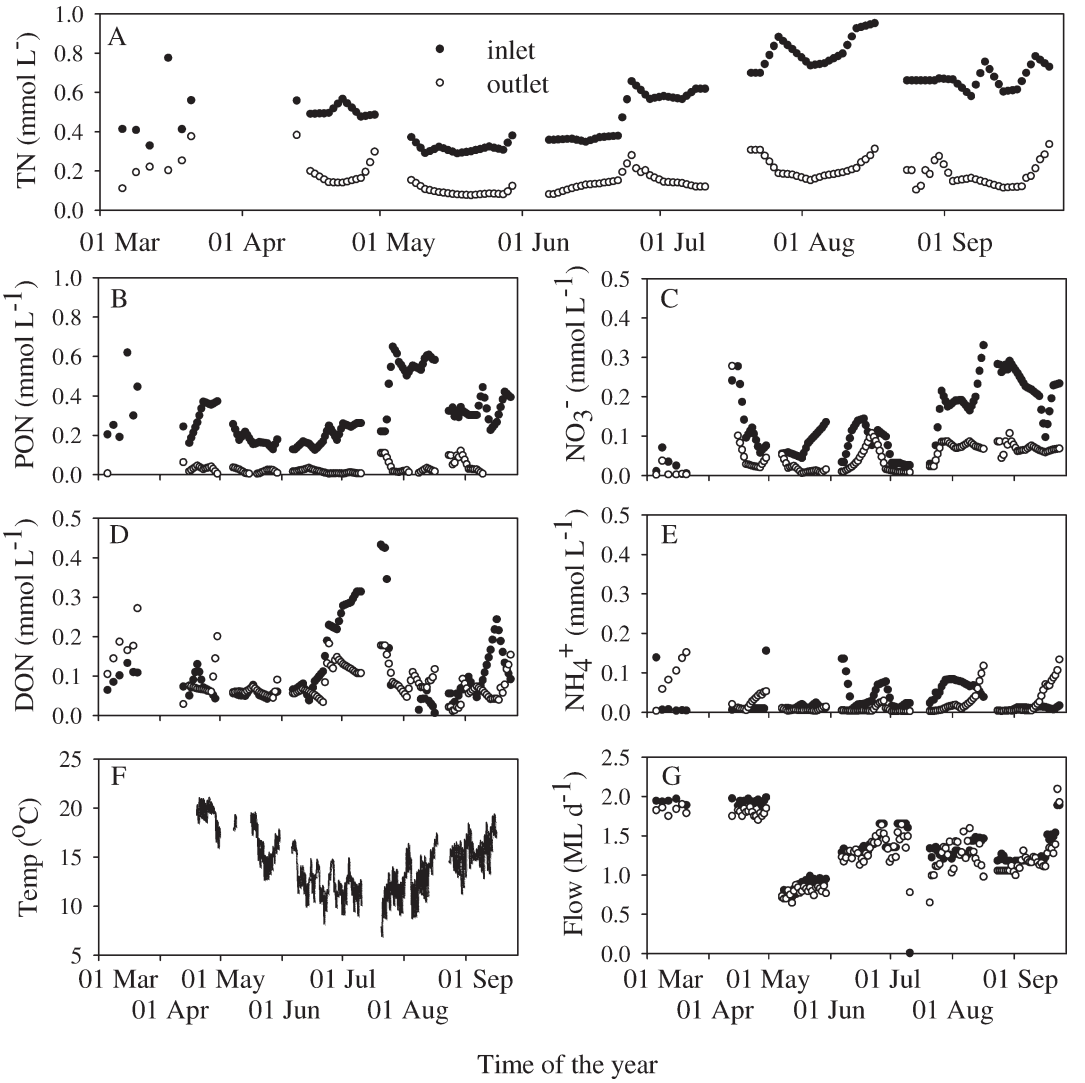

Fig. 3. Long-term (7 months, March–September 2007) nutrient, temperature, and flow data for the Casino constructed wetland cell B. (A) TN, (B) PON, (C) NO_3^-, (D) DON, (E) NH_4^+, (F) temperature, and (G) flow.

The NH_4^+ and excess $^{15}NH_4^+$ concentrations (Fig. 4C,D) were consistently greater within the wetland relative to inlet water and show a distinct peak at the MDs, and to a lesser degree, at the outlet, corresponding to the peak in Li^+ concentration. A second peak is observed on the following day corresponding to the second tracer release (note there was no Li added in the second release). The NH_4^+ concentrations increased over the inundation period at the MDs and the outlet. For excess $^{15}NH_4^+$, concentrations at the MDs dropped from 91.5 nmol L^{-1} during the enrichment to 4.8 nmol L^{-1} on day 2. There were two peaks of release at the MDs before the dry-out period, one on day 8 (10.0 nmol L^{-1}) and one on day 14 (9 nmol L^{-1}) (Fig. 4D inset). The same pulses were not recorded at the outlet. There was also a small spike in NH_4^+ (Fig. 4C) and excess $^{15}NH_4^+$ concentration immediately after the start of the second inundation phase (day 26) (Fig. 4D inset).

The PON concentrations during the whole-system addition experiment show that 49.8% ± 0.9% of the PON in the influent water was removed before the MDs (Fig. 4E). By the time water had reached the wetland outlet, 88.3% ± 1.4% of inlet PON was removed from the water. Of the added $PO^{15}N$, 48.2% ± 4.2% had been removed between the inlet and the MDs and 92.2% ± 6.2% had been removed between the inlet and the outlet. There were spikes in PON and excess $PO^{15}N$ concentration corresponding to the two tracer releases at the MDs (Fig. 4E,F). There were also spikes in PON and excess $PO^{15}N$ concentration immediately after the start of the second inundation phase at the MDs and the outlet (Fig. 4F inset).

The NO_3^- concentrations in the wetland water were consistently reduced between inlet and MDs and the MDs and the outlet (Fig. 4G). The excess $^{15}NO_3^-$ concentration at the MDs shows two distinct peaks corresponding to the tracer releases, followed by a third peak 2 d after the last tracer release and lasting until day 5 (Fig. 4H). In contrast the excess $^{15}NO_3^-$ concentration never exceeded 16 nmol L^{-1} at the wetland outlet. There was a small spike in NO_3^- and excess $^{15}NO_3^-$ concentration immedi-

Table 3. Change in N species concentration (Conc.). and stable-isotope ratio ($\Delta\delta^{15}N$) during the two tank stable-isotope enrichments (E1 and E2), and excess ^{15}N concentrations of wetland influent water and the total amount of ^{15}N added to the wetland during the two stable-isotope releases.

	Tank enrichments			Wetland inflow including enriched plume			
	Conc. before (μmol L^{-1})	Conc. after (μmol L^{-1})	$\Delta\delta^{15}N$ (‰)	Conc. (μmol L^{-1})	$\Delta\delta^{15}N$ (‰)	Excess ^{15}N (μmol L^{-1})	^{15}N (mol)
E1							
NH_4^+	2	106	1.3×10^7	4	3.2×10^5	2.25	0.23
NO_3^-	307	282	1.0×10^4	306	2.4×10^2	0.23	0.02
PON	385	410	6.2×10^4	490	1.2×10^3	2.11	0.22
DON	64	202	1.0×10^4	67	7.2×10^2	0.16	0.01
E2							
NH_4^+	2	113	8.8×10^6	3	2.1×10^5	1.40	0.23
NO_3^-	290	290	1.0×10^4	461	1.7×10^2	0.23	0.03
PON	385	394	5.1×10^4	613	6.4×10^2	1.34	0.22
DON	64	212	7.4×10^3	105	3.7×10^2	0.12	0.02

ately after the start of the second inundation phase (Fig. 4G,H).

The DON concentration profiles showed no distinct trend with inlet and MD concentrations, displaying wide variability (Fig. 4I). In this study, a new method for $DO^{15}N$ analysis was used. The results show that the method worked well for standards containing ^{15}N-labeled urea (measured values were within ± 2‰ of the actual values). However water samples from the whole-system trial showed large variability in excess $DO^{15}N$ concentrations between sample replicates. Nevertheless, increase in the excess $DO^{15}N$ concentration at the wetland outlet was observed during the first week following tracer addition (*see* Fig. 4J), after which excess $DO^{15}N$ concentration at the wetland outlet appeared to approach zero. The high variability in the $DO^{15}N$ method could have obscured the tracer N signal.

Tracer N transformations, distributions, and mass balance—An isotope mass balance was constructed to estimate the rates of NH_4^+ uptake and production (mineralization) and NO_3^- uptake and production (nitrification). Uptake of the available NH_4^+ was 23 ± 15 μmol m^{-2} h^{-1} in subcell B1 relative to 100 ± 50 μmol m^{-2} h^{-1} in subcell B2. The rate of mineralization of NH_4^+ appeared to be greater in subcell B1 relative to B2 (154 ± 25 and 55 ± 45 μmol m^{-2} h^{-1}, respectively). The rate of NO_3^- uptake was 1280 ± 120 μmol m^{-2} h^{-1} in subcell B1 compared to B2, which was 1050 ± 50 μmol m^{-2} h^{-1}. The percentage removal of NO_3^- was 52.1% and 99.9% in subcells B1 and B2, respectively. Net production of NO_3^- (nitrification) was positive in subcell B1 (3 ± 2 μmol m^{-2} h^{-1}) and accounted for 14.6% ± 4.2% of the NH_4^+ uptake. In subcell B2, the rate of net nitrification could not be calculated because of the high rate of NO_3^- uptake (i.e., there was no net production of $^{15}NO_3^-$).

The quantity of ^{15}N stored in the sediment and macrophyte pools changed over the course of the whole-system tracer-addition experiment (Fig. 5). Initially, the bulk of the added ^{15}N was found in sediments close to the wetland inlet (sampling location 1; Fig. 5A). Over the 4-month sampling period, ^{15}N in the sediments generally showed a downstream migration until the bulk of the ^{15}N was located at sampling location 7 (Fig. 5F). Statistical analysis revealed that there was a significant difference in the sediment excess ^{15}N over time ($F_{5,10} = 2.91$, $p < 0.05$, $n = 3$), and there was also a significant difference in the sediment excess ^{15}N at the different sites over time ($F_{30,42} = 3.81$, $p < 0.01$, $n = 3$). Macrophyte tissue did not incorporate significant amounts of the added ^{15}N until 2 weeks after the tracer release (Fig. 5G–L). The macrophyte excess ^{15}N was stable between day 15 and day 45 (≈ 0.26 mol ^{15}N) but had declined by day 157 (0.06 mol ^{15}N). Statistical analysis revealed that there was a significant difference in macrophyte excess ^{15}N over time ($F_{5,10} = 23.2$, $p < 0.01$, $n = 3$), and there was also a significant difference at different locations over time ($F_{30,42} = 2.6$, $p < 0.01$, $n = 3$).

Estimates of the distribution of added tracer ^{15}N in the various wetland pools over the entire sampling period, and the percentage removal of added ^{15}N, are shown in Fig. 6A,B. The wetland removed 95% ± 25% of the added ^{15}N within the first 2 d after tracer addition. Again, the sediments are shown to be the major sink for N, initially removing 78% ± 18% of the added ^{15}N. There is a gradual decline in sediment ^{15}N until day 157. Macrophyte storage initially removed 8.2% ± 2.4% of the added ^{15}N. This increased to 26% ± 6% by day 14 and remained at this level until day 43. The amount of ^{15}N released as $^{15}NH_4^+$ from the wetland in the first 2 d was 3.1% ± 0.7%. By day 15, 7.3% ± 0.2% of the added tracer had been lost from the wetland as $^{15}NH_4^+$, and by day 32, the value was 15% ± 3.5%. Pore water remained enriched in ^{15}N up until day 43, and the maximum amount of ^{15}N stored in pore water was 4.0% ± 1.9% of the added ^{15}N (found on day 32). At the end of the 157-d sampling period, the storage of ^{15}N in sediments was 30% ± 7.3% and macrophyte storage accounted for 7.4% ± 3.8 %. The amount of $^{15}NH_4^+$ exported from the wetland via the outlet was 15% ± 3.7% of the total added ^{15}N. The total amount of ^{15}N exported from the wetland was 18% ± 3.8% of the total added ^{15}N. By day 157, the amount of unaccounted ^{15}N, which is assumed to be lost to the atmosphere as $^{15}N_2$, was 40% ±

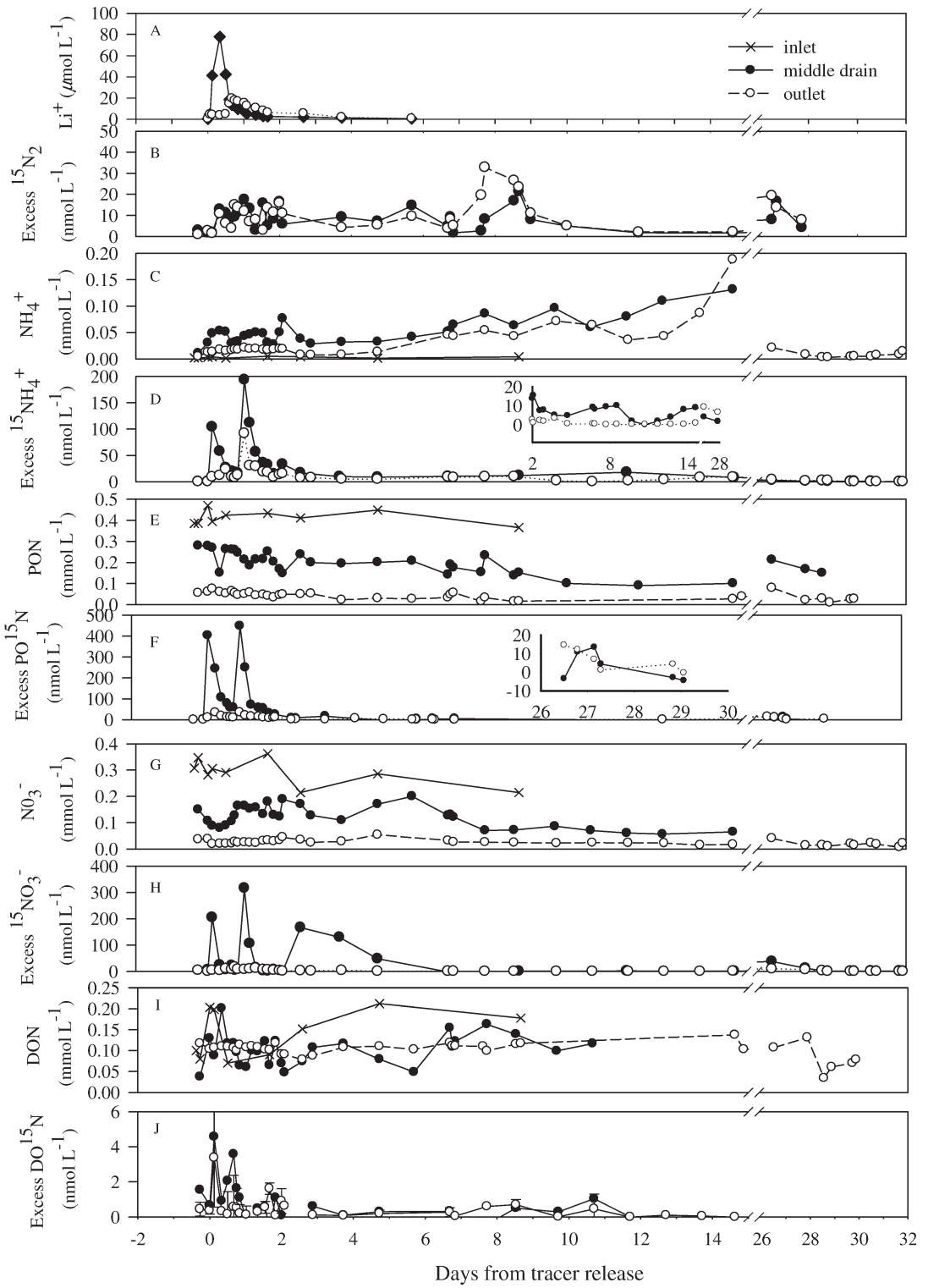

Fig. 4. Lithium, nitrogen, and excess ^{15}N concentrations during the first 32 d (representing the inundation phase) of the whole-system stable-isotope-addition experiment. The experiment was conducted shortly after the 7-month monitoring period in Fig. 2. (A) Lithium, (B) excess $^{15}N_2$, (C) NH_4^+, (D) excess $^{15}NH_4^+$, (E) PON, (F) excess $PO^{15}N$, (G) NO_3^-, (H) excess $^{15}NO_3^-$, (I) DON, and (J) excess $DO^{15}N$. The break in the *x*-axes (days 15–25 omitted) was the dry-out phase. The inset in the fourth panel represents a close-up view of excess $^{15}NH_4^+$ concentrations between days 2 and 28 (with days 15–25 omitted); the inset in the sixth panel represents a close-up view of excess $PO^{15}N$ concentrations immediately after the end of the dry-out phase.

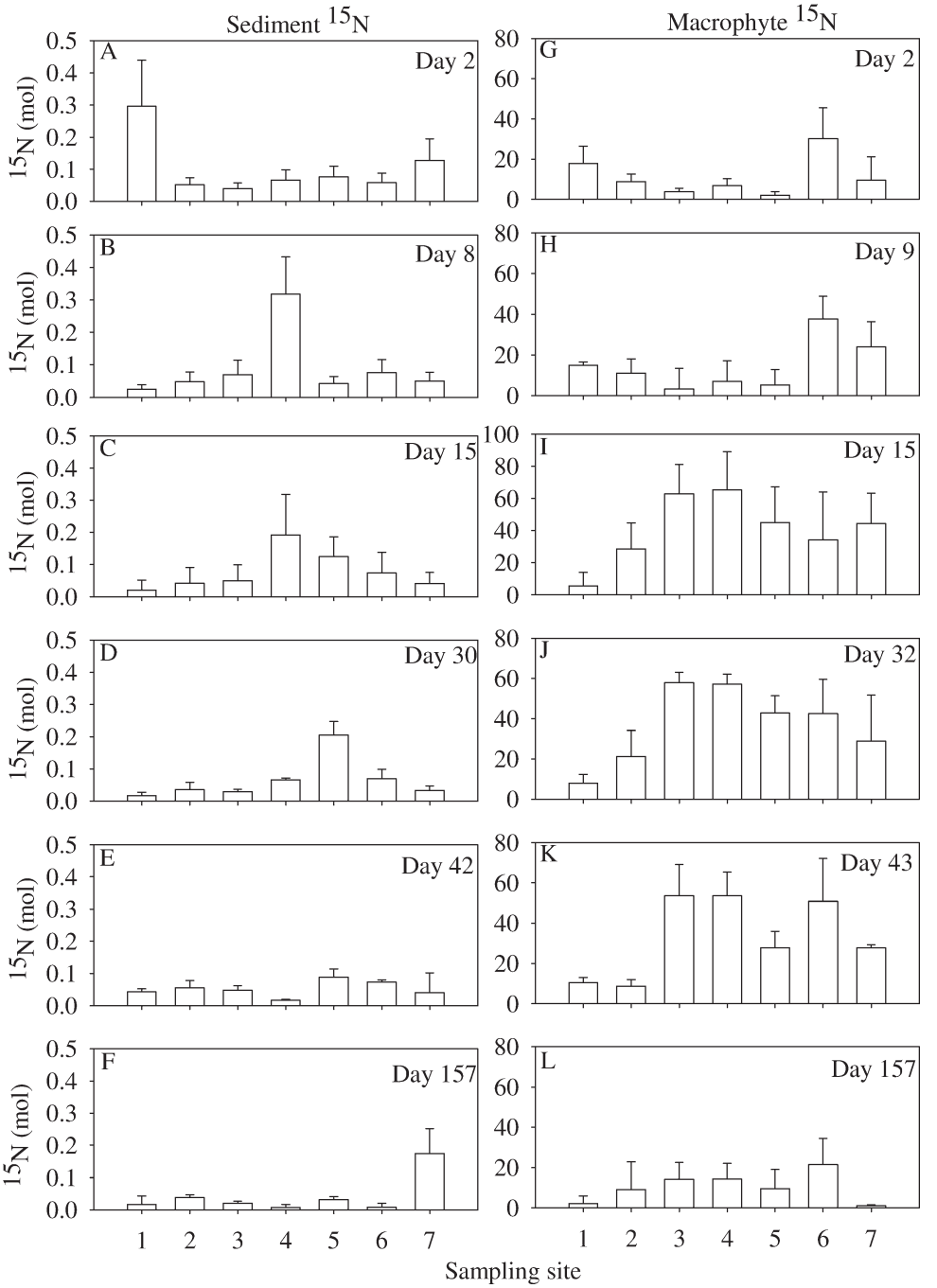

Fig. 5. Sediment and macrophyte excess ^{15}N content in the wetland (sites 1–7) during the first 157 d of the whole-system isotope-tracer-addition experiment.

9.1% of the total added ^{15}N. The actual amount of $^{15}N_2$ measured in the wetland outlet water over the entire sampling period accounted for 13.5% ± 3.2% of the total added ^{15}N. While the main N_2 production mechanism in the Casino constructed wetland is denitrification, significant input from anammox is known to occur (Erler et al. 2008). For the sake of brevity, we refer to N_2 production as denitrification throughout the text, but it must be noted that other N_2 production pathways also exist.

Core incubations—During the core incubations, there was a clear shift in the quantity of $^{15}NH_4^+$ and $^{15}NO_3^-$ being effluxed to the water overlying wetland sediments. In the first incubation, conducted 10 d after tracer release, the sediments from all sampling sites effluxed $^{15}NH_4^+$ (Fig. 7A). The highest effluxes were at sampling site 1, followed by sampling sites 5 and 7. There was negligible efflux of $^{15}NO_3^-$, except at sampling site 6, where there was an unexpected efflux of 18.6 ± 2.2 nmol m^{-2} h^{-1} (Fig. 7A). The

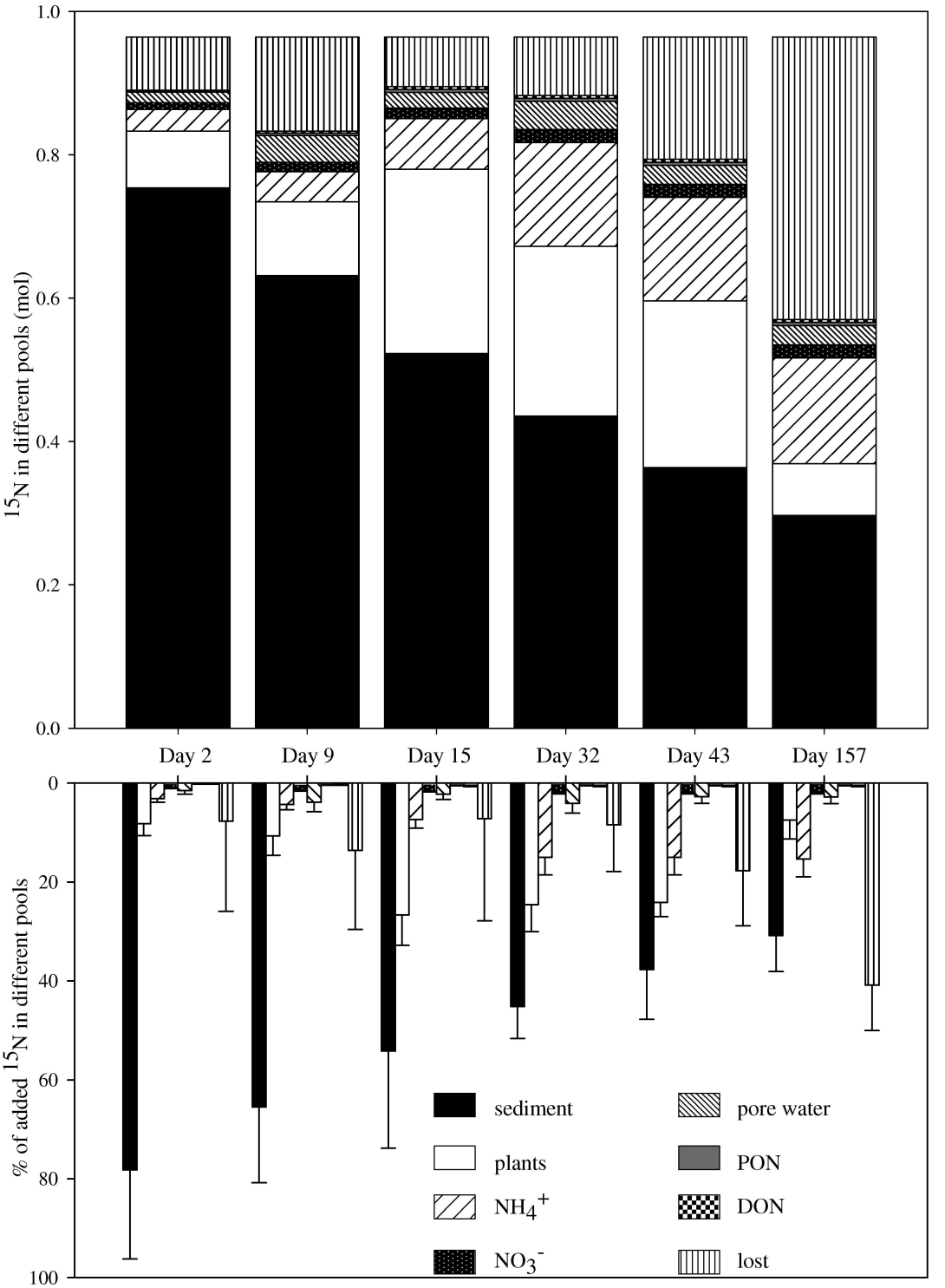

Fig. 6. Distribution of added ^{15}N in various compartments during the first 157 d of the whole-system stable-isotope-addition experiment expressed as a stacked bar chart showing the quantity of ^{15}N in the different wetland pools (upper panel) (note that 'lost' represents excess ^{15}N that was unaccounted for, presumably lost as N gas emissions). The lower panel shows the individual measurements with standard errors (SE).

production of $^{15}N_2$ was detected at all sampling sites and was highest at site 1 (Fig. 7A). Dissolved oxygen uptake averaged 5.3 ± 0.7 mmol m^{-2} h^{-1} in the upstream cores and 5.5 ± 0.5 mmol m^{-2} h^{-1} in the downstream cores.

During the second core incubation, conducted during the dry-out phase, there were appreciable $^{15}NO_3^-$ effluxes at sites 1, 4, and 6 (Fig. 7B). There were no appreciable effluxes of $^{15}NH_4^+$ (Fig. 7B). There was a positive efflux of

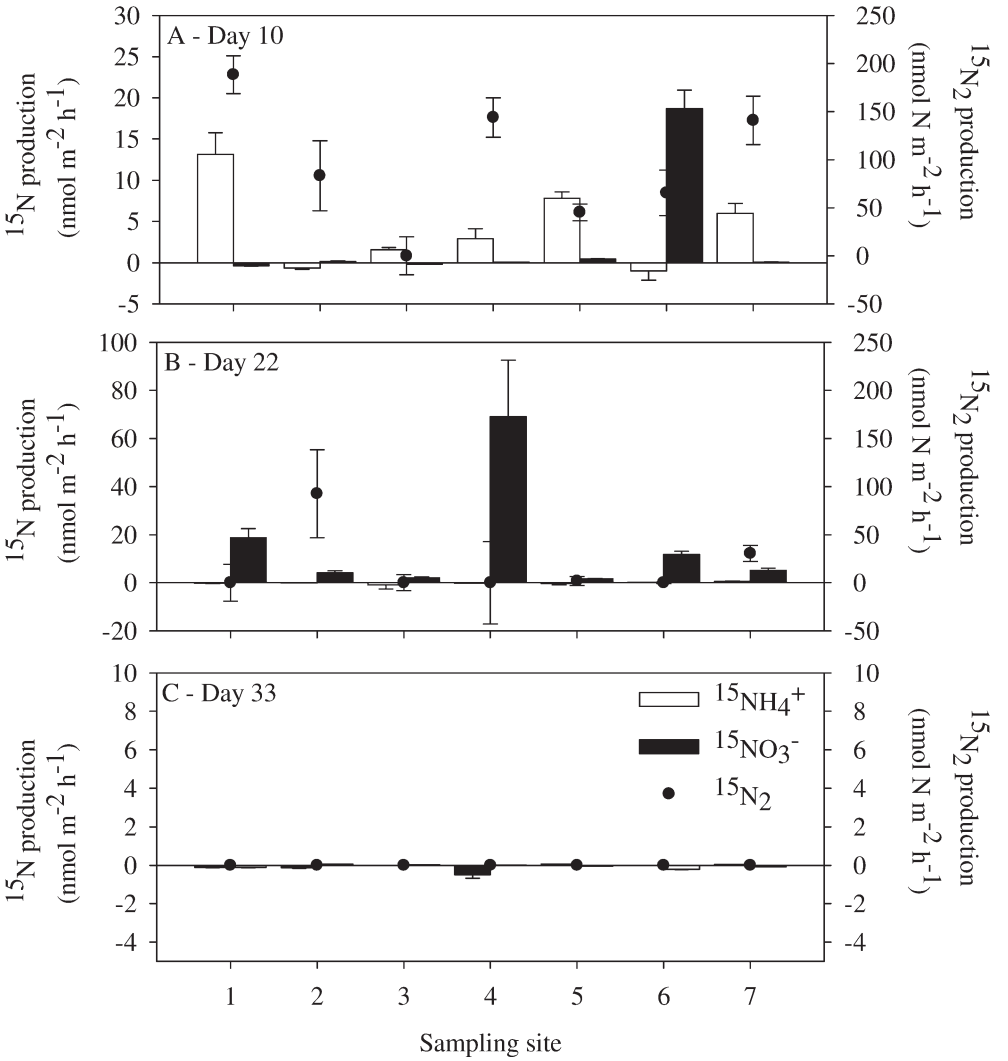

Fig. 7. The production of $^{15}N_2$, $^{15}NH_4^+$, and $^{15}NO_3^-$ during the three core incubations (A, B, and C, respectively) at the seven wetland sites.

$^{15}N_2$ at sites 2 and 7 during the second incubation. Dissolved oxygen uptake averaged 2.7 ± 0.4 mmol m^{-2} h^{-1} in the upstream cores and 3.0 ± 0.5 mmol m^{-2} h^{-1} in the downstream cores. The final core incubation, conducted 33 d after tracer release, failed to yield any measurable efflux of $^{15}NH_4^+$, $^{15}NO_3^-$, or $^{15}N_2$ (Fig. 7C).

Discussion

Very short-term N behavior (1–2 d)—Very short-term behavior is described here as the fate of inlet N within a period of twice the hydrological residence time of the wetland. Overall, there was very high removal of added ^{15}N (≈ 95%) during the first 2 d after tracer addition. The removal of PON was the dominant process: 92% of PO^{15}N was trapped in the wetland. The bulk of the removed PO^{15}N evidently settled to the sediments in the intake zone (site 1, *see* Fig. 5A), highlighting the physical sedimentation and filtration capacity of the wetland. As well as particulate removal, there was also rapid, and spatially variable, cycling of inorganic N in the very short term. This rapid cycling is described with the conceptual model presented in Fig. 8.

In the upstream section of the wetland (subcell B1, Fig. 8), there were threefold higher rates of NH_4^+ mineralization relative to rates in the downstream section. The rate of NH_4^+ influx via inlet water was low compared to mineralization and does not appear to have significantly influenced N cycling. Mineralization in the upstream section most likely resulted from the mineralization of PON initially removed from the inlet water. This makes sense in light of the high PO^{15}N removal observed in subcell B1 in the very short term. The bulk of the mineralized NH_4^+ was passed to the downstream region of the wetland. Inlet NH_4^+ was also assimilated into plant tissue (9–40% of the assimilated NH_4^+) and also into microbial biomass (Fig. 8). The other pathway of NH_4^+ uptake was nitrification; however, only a small fraction of

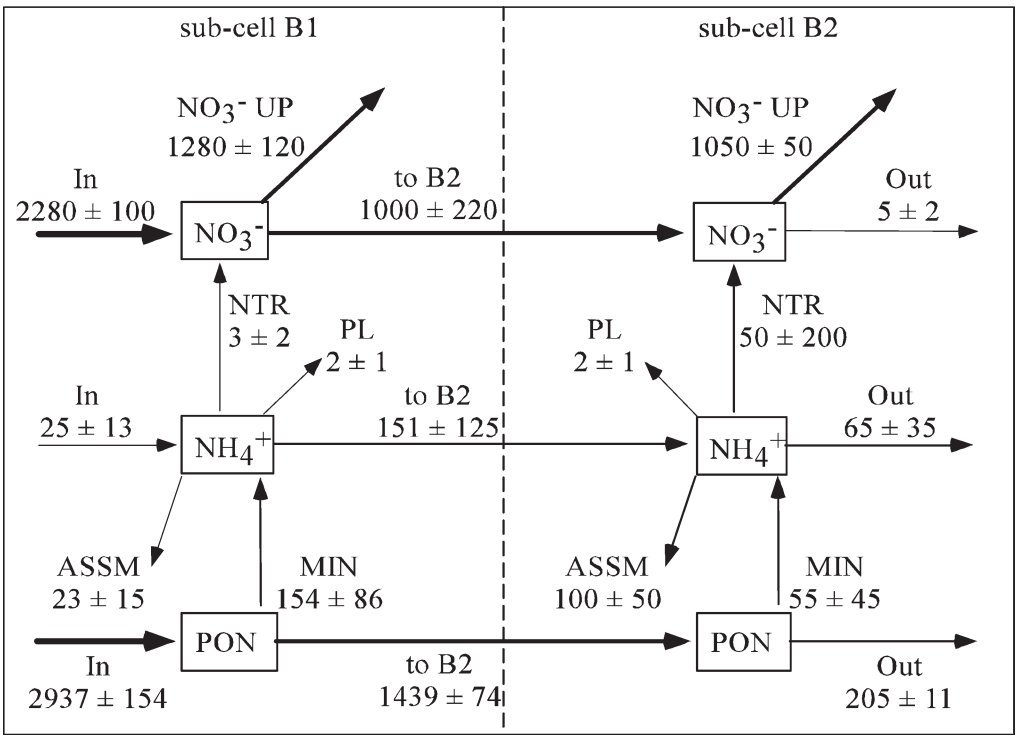

Fig. 8. Conceptual model of very short-term N cycling (μmol m^{-2} h^{-1}) within the studied wetland; NO_3^- UP is the net uptake rate of NO_3^-, NTR is the rate of nitrification, PL is the rate of plant uptake, and ASSM and MIN are the rates of NH_4^+ assimilation and mineralization, respectively. Line thickness provides an indicative comparison of rate.

the inlet NH_4^+ was converted to NO_3^-. Nitrification therefore does not appear to have been a significant contributor to the NO_3^- pool in the upstream (B1) section.

In the downstream section of the CW, there appears to be less mineralization of NH_4^+ but higher rates of NH_4^+ assimilation and nitrification relative to the upstream section. The reduced mineralization would make sense in light of the reduced PON settlement in the downstream region. However, the higher uptake rates are more difficult to explain. Using the amount of ^{15}N found in macrophyte tissue as a percent of the inlet $^{15}NH_4^+$, the rate of plant uptake can be estimated (*see* Fig. 8). This rate was similar between upstream and downstream regions. If plant uptake and nitrification are subtracted from the total NH_4^+ uptake rates, the total assimilation rate is 100 ± 50 μmol m^{-2} h^{-1} downstream relative to an upstream rate of 20 ± 10 μmol m^{-2} h^{-1}. Explanations for higher rates of NH_4^+ assimilation in the downstream relative to the upstream region of the wetland include greater rates of microbial assimilation or the presence of active but undetected nitrification.

The rates of uptake of NO_3^- exceed all other N transformations in both the upstream and downstream sections of the wetland. In the upstream section, NO_3^- uptake removed 56% of the available NO_3^-, leaving the remainder to flow into the downstream region of the wetland. In the downstream region, NO_3^- uptake removed all of the available NO_3^-. In fact, there was a 0.05 mmol m^{-2} h^{-1} deficit of NO_3^- that can only be supplied through nitrification. As mentioned in the results section, the rate of nitrification could not be estimated downstream because $^{15}NO_3^-$ was completely removed from the water column. However, the estimation of nitrification by difference indicates a rate of 0.05 ± 0.2 mmol m^{-2} h^{-1} in the downstream region. The high error associated with this figure reflects the cumulative errors involved in the calculation.

The estimated rate of nitrification for the downstream region was greater than the measured rate in the upstream region and would seem counterintuitive given the low dissolved oxygen concentrations in subcell B2. Unfortunately, no core incubation was conducted in the very short term to estimate rates of nitrification, but $^{15}NO_3^-$ production was detected at sampling site 6 in the 10-d core incubation. Ex-situ mesocosm experiments in this wetland have also shown nitrification to occur in the downstream regions down to DO concentrations of 30 μmol L^{-1} (D. V. Erler unpubl. data). This is well above the reported threshold for nitrifiers of 5 μmol L^{-1} (Canfield et al. 2005). Therefore, we postulate that nitrification does occur in the downstream region of the wetland, despite the low dissolved oxygen concentrations found there.

In summary, the mass-balance model of nutrient dynamics in Fig. 8 depicts the very short-term cycling of inorganic N. Spatial variability in the rates of NH_4^+ mineralization and uptake, however, is somewhat dwarfed by the high rate of NO_3^- uptake. In the very short term, there is also a large removal of PON, the eventual fate of which is discussed later herein.

Short-term behavior (1–2 weeks)—In the short term, there was a downstream movement of the ^{15}N initially removed from the water column at site 1. This ^{15}N was recovered in the sediments of site 4 and also in macrophyte

tissue in the middle to downstream regions of the wetland (i.e., sites 3–7) (Fig. 5). The transfer of N from pool to pool appears to be critical in retaining N within the wetland. However, between mineralization and assimilative uptake, DIN is susceptible to advective loss from the wetland. This was observed toward the end of the short-term period (14 d) as an increase in NH_4^+ concentrations at both MD and the outlet (Fig. 4C). In addition, the mineralization of sediment ^{15}N in the short term appears to have led to an increase in the excess $^{15}NH_4^+$ concentration at the MDs toward the end of the inundation phase (Fig. 4D inset). This is an important observation because it demonstrates that wetland uptake of PON can be compromised by the eventual mineralization and release of N to downstream waters. The loss of NH_4^+, particularly toward the end of the treatment cycle, was also observed in the long-term monitoring data (Fig. 3E). In particular, during the end of the last two inundation phases, there was a noticeable increase in NH_4^+ concentration at the wetland outlet.

The conceptual model presented in Fig. 8 shows that NH_4^+ mineralization occurs within the upstream and downstream regions of the wetland. Using the mass balance in Fig. 6, it is possible to roughly estimate the age of the released NH_4^+. The amount of $^{15}NH_4^+$ released from the wetland between day 2 and day 14 was $\approx 8\%$ of the added PO^{15}N. If we extrapolate this to the amount of PON entering the wetland (i.e., ≈ 2.8 mmol m^{-2} h^{-1}), we can estimate that 228 μmol m^{-2} h^{-1} of the total mineralized NH_4^+ is derived from PON deposited up to 2 weeks prior. This is close to the maximum total amount of NH_4^+ mineralized in the wetland, which is the sum of the maximum mineralization in each region (i.e., ≈ 304 μmol m^{-2} h^{-1}). This implies that by day 14, the N initially removed to the sediments as PON is being actively mineralized back to the wetland water.

Further evidence of the internal recycling of N within the short term can be seen by a close examination of the $^{15}NO_3^-$ dynamics. On day 3 after tracer release, a pulse in excess $^{15}NO_3$ concentration can be seen at the MDs. This pulse lasts until day 6 and also precedes a minor elevation of labeled $^{15}N_2$ at the MDs and the outlet (Fig. 4B). The first core incubation also shows that there is a loss of labeled $^{15}N_2$ from the sediments lasting longer than the hydraulic residence time of the CW. Interestingly, in the first core incubation, there was a significant production of NO_3^- from the downstream site 6. This further supports the earlier presumption of nitrification in the downstream region of the wetland. Other evidence that demonstrates the continued transformations of initially removed N is the small pulse of $^{15}NH_4^+$ and $^{15}N_2$ on day 9 (Fig. 4C,D inset). The presence of these labeled species in the wetland water indicates that initially absorbed N is being mobilized from the sediments and that this gradual release of N from the sediments allows for greater loss of N via N_2 production.

The initial retention, eventual mineralization, and subsequent transformations of N increase the opportunity for loss via processes such as denitrification. This type of N spiraling has been observed in wetland mesocosms (Kadlec et al. 2005) but never at the whole-ecosystem scale in wetlands.

Medium-term behavior (2–8 weeks)—The medium term encapsulates a complete wetland treatment cycle, i.e., a flood phase, a dry-out phase, and the start of another flood phase. In the medium term, we observed a continuing downstream movement of sediment and macrophyte ^{15}N, again emphasizing the process of N spiraling in the wetland (Fig. 5). Overall, macrophyte excess ^{15}N was stable during the medium term, but there was a reduction in sediment excess ^{15}N and a corresponding increase in the amount of N lost from the system. This suggests that the macrophyte is a stable storage pool for N in the medium term, whereas the sediment pool is more reactive.

An important part of many CW treatment cycles is the dry-out phase. Operators of the wetland in this study routinely dry-out wetland cells, believing that it allows the wetland sediments to aerate, encourage PON oxidation, and improve the nitrification and denitrification potential of N trapped during the inundation phase. While a number of studies have looked at wetland N removal during inundation, fewer studies have looked at N transformation during a dry-out phase. In this study, core incubations were conducted during the dry-out phase to try and identify the dominant N cycling processes. During this incubation $^{15}NO_3^-$ was the dominant ^{15}N species produced, compared to $^{15}NH_4^+$, which is generally produced during the inundation phase. There was less DO uptake in the dry-out phase incubation, reflecting the unsaturated nature of the sediments. The DO uptake was higher in the inundation phase incubation, possibly as a result of anoxia in the sediments, stripping DO from the water column. These trends suggest that there was enhanced nitrification of $^{15}NH_4^+$ stored in the pore water or mineralized from PO^{15}N upon desiccation. There was a high relative rate of $^{15}N_2$ production measured at site 2 and only small amounts of $^{15}NH_4^+$ detected in the dry-out phase incubation. These results show that the dry-out phase can potentially enhance nitrification in wetland sediments. This nitrification should lead to the production of N_2, via denitrification, at the onset of the ensuing inundation phase, and it appears to be a valid option for facilitating permanent removal of reactive N wetlands. To quantify N transformations in the second inundation phase, a third core incubation was performed. This time, there were no detectable ^{15}N fluxes, suggesting that all labile PO^{15}N had been completely transformed within 33 d of its retention in the wetland.

At the start of the second inundation phase (day 24), a small pulse of PON and PO^{15}N was detected at the MDs and the outlet (Fig. 5E,F inset). There were also small pulses of NO_3^-, $^{15}NO_3^-$, NH_4^+, and $^{15}NH_4^+$ at the start of the inundation phase. The release of nutrients, albeit relatively minor, during the early part of the inundation supports the concept of scouring or wash-out (Davidsson and Stahl 2000) associated with the initial movement of water through the wetland following the dry-out phase.

The dynamics of DON in constructed wetlands remain largely understudied because of the difficulties associated with DO^{15}N analysis. In this study, the DON concentration was largely unchanged between wetland inlet and outlet. However, the appearance of enriched DO^{15}N strongly

Table 4. Percentage removal and storage of N within different constructed wetland nutrient pools. Type refers to the type of study (MB, mass balance; MC, mesocosm CW; C, core incubations; NA, natural abundance stable isotope; WS, whole-system stable isotope).

Sediment N	Macrophyte	N_2 loss	Outlet N	Time	Type	Study
—	27–47	—	—	3 yr	MB	Greenway and Woolley (2001)
24–26	11–15	61–63	—	32 d	MC	Matheson et al. (2002)
	20–25	77–95	—		MC	Ruckauf et al. (2004)
28–37	6–48	≈1	—	120 d	MC	Kadlec et al. (2005)
2	—	25	—	8 months	NA	Reinhardt et al. (2006)
50	—	—	—	11 months	C	Scott et al. (2008)
31±7	7±4	41±8	18±4	157 d	WS	This study

suggests that the constitution of the DON pool did change as water passed through the wetland. As mentioned earlier, DON constitutes the largest fraction of N in the wetland outlet. Attempts to improve N removal in wetlands should focus on DON oxidation to inorganic N, which can then be subject to permanent removal via denitrification.

Long-term behavior (≈ 6 months)—The longer term behavior of the wetland is best described by the mass balance (Fig. 6), wherein the major N storage pool in the wetland is the sediment, which retained around 30% of added ^{15}N by day 157. Macrophytes retained roughly 7.5% of the added ^{15}N by the end of the measurement period. The amount of ^{15}N retained in sediments remained relatively stable between day 45 and day 157. We hypothesize that the stability of the sediment N pool in this period was not a result of reduced sediment N mineralization, but rather reflects a balance between the addition of macrophyte tissue N to the sediment and the loss of N from the sediment through N_2 production and mineralization. It appears as though macrophyte N enters the sediment N pool, where the N eventually becomes subject to gaseous loss and is also released to the water column as DIN. The net result is a relatively stable sediment N pool size at dynamic steady state.

In this study, the bulk of added ^{15}N (≈ 41%) could not be accounted for and is considered lost to the atmosphere as gaseous N. The use of unaccounted ^{15}N as an estimate of atmospheric loss is not ideal given that this residual value is affected by the cumulative errors of other flux measurements. Independent estimates of N loss are required to support the assumption that gaseous N loss explains the unaccounted N. One way of calculating gaseous N loss is to multiply the excess $^{15}N_2$ concentration data in the wetland outlet water by the volume of water discharged. This yields a figure of 0.12 ± 0.02 mol of ^{15}N, or 13.5% ± 3.2% of the total added ^{15}N, lost as dissolved $^{15}N_2$ in the first 30 d of the trial. However, because this estimate can only be made for the first 30 d of the trial (beyond that, the concentration of $^{15}N_2$ was too low to be detected in the outlet water), it underestimates the true value. At best, it describes the minimum amount of added ^{15}N lost as $^{15}N_2$ from the CW.

Another approach is to extrapolate the core incubation $^{15}N_2$ production rates to the entire wetland. However, the core incubations do not accurately reflect in-situ oxygen or redox conditions. Nevertheless, for this exercise, it is best to use the $^{15}N_2$ production rates from the first core incubation because the most appreciable N_2 flux occurred during that incubation. If we assume that this production of N from the wetland is permanent (i.e., no fixation of the N_2), and that the efflux measured during the first core incubation is constant for the first 10 d after tracer addition, then our results show that in the first 10 d, up to 0.14 ± 0.10 mol of added ^{15}N (or 15% ± 4%) was potentially lost to the atmosphere. This value agrees well with the mass-balance estimate of ^{15}N lost after 9 d (0.12 ± 0.14 mol). However, the efflux of $^{15}N_2$ would clearly not be constant over the first 10 d of the experiment, and, unfortunately, there was no core incubation performed before day 10. Accepting the uncertainties of the core incubations, we now have two estimates of N loss via N_2 production that are in rough agreement.

As a comparison, Table 4 reports N removal rates measured in other constructed wetland studies. The comparison includes two published studies, in addition to the present one, that show that the major N storage pool in wetlands appears to be the sediment rather than plant macrophytes. The principal role of macrophytes in wetlands, however, may be to facilitate aerobic sediment processes such as nitrification rather than to remove and store N (Matheson et al. 2002). Macrophytes must also increase residence time and help trap particulate organic matter, and where labile organic matter is not abundant in the source water, they must also be important in driving denitrification (which, according to the Table 4, can remove up to 95% of inlet N from wetlands).

In conclusion, this study is the first to quantify both the temporal and spatial N transformations in a full-scale wetland. In the very short term, particulate N is physically removed to wetland sediments, and NO_3^- from the inlet water is removed along the flow path. There is mineralization of NH_4^+, which is more pronounced in the upstream section of the wetland, and we estimate that this mineralized N had been assimilated 14 days prior. Nitrification is active in the downstream regions of the wetland despite the low dissolved O_2 concentrations there. The major DIN removal pathway was denitrification, and the rate was similar within the wetland. In the short term, N was transferred into sediment and macrophyte pools over much longer timescales than the hydrologic residence time, offering enhanced opportunity for permanent removal as denitrification. In the medium and long term, the bulk of the N was lost through denitrification and accumulated into sediments. Disturbance associated with wetland dry-out showed some enhancement of sediment nitrification and resulted in a minor wash-out of N during the next

inundation cycle. Overall, we have demonstrated that internal recycling retards the flow of N through wetlands, facilitating improved assimilation and removal.

Acknowledgments

We thank our industry partners Ecotechnology Australia, Ecotech Group, and the Ballina, Byron Bay, and the Richmond Valley Shire Councils. We also thank technical staff at the School of Environmental Science and Management, Southern Cross University, and the reviewers for their instructive and helpful feedback. This project was supported by an Australian Research Council (ARC) Linkage grant (LP0667449), ARC Discovery grants (DP0663159, DP0878568), and ARC LIEF grant (LE0668495) awarded to B.E.

References

Burgin, A. J., and S. K. Hamilton. 2008. NO_3-driven SO_4^{2-} production in freshwater ecosystems: Implications for N and S cycling. Ecosystems **11:** 908–922, doi:10.1007/s10021-008-9169-5

Cameron, K., C. Madramootoo, A. Crolla, and C. Kinsley. 2003. Pollutant removal from municipal sewage lagoon effluents with a free-surface wetland. Water Res. **37:** 2803–2812, doi:10.1016/S0043-1354(03)00135-0

Canfield, D. E., B. Thamdrup, and E. Kristensen. 2005. Aquatic geomicrobiology. Elsevier.

Cloern, J. E. 2001. Our evolving conceptual model of the coastal eutrophication problem. Mar. Ecol. Prog. Ser. **210:** 223–253, doi:10.3354/meps210223

Davidsson, T. E., and M. Stahl. 2000. The influence of organic carbon on nitrogen transformations in five wetland soils. Soil Sci. Soc. Am. J. **64:** 1129–1136.

———, R. Stepanauskas, and L. Leonardson. 1997. Vertical patterns of nitrogen transformations during infiltration in two wetland soils. Appl. Environ. Microb. **63:** 3648–3656.

Erler, D. V., B. D. Eyre, and L. Davison. 2008. The contribution of anammox and denitrification to sediment N_2 production in a surface flow constructed wetland. Environ. Sci. Techn. **42:** 9144–9150, doi:10.1021/es801175t

Eyre, B. D., and A. J. P. Ferguson. 2005. Benthic metabolism and nitrogen cycling in a subtropical east Australian estuary (Brunswick): Temporal variability and controlling factors. Limnol. Oceanogr. **50:** 81–96.

Fry, B. 2005. Stable isotope ecology. Springer.

Greenway, M., and A. Woolley. 2001. Changes in plant biomass and nutrient removal over 3 years in a constructed wetland in Cairns, Australia. Water Sci. Technol. **44:** 303–310.

Gribsholt, B., and others. 2005. Nitrogen processing in a tidal freshwater marsh: A whole-ecosystem N-15 labeling study. Limnol. Oceanogr. **50:** 1945–1959.

Holmes, R. M., J. W. McClelland, D. M. Sigman, B. Fry, and B. J. Peterson. 1998. Measuring $^{N15}NH_4^+$ in marine, estuarine and fresh waters: An adaptation of the ammonia diffusion method for samples with low ammonium concentrations. Mar. Chem. **60:** 235–243, doi:10.1016/S0304-4203(97)00099-6

Ishida, C. K., J. J. Kelly, and K. A. Gray. 2006. Effects of variable hydroperiods and water level fluctuations on denitrification capacity, nitrate removal, and benthic-microbial community structure in constructed wetlands. Ecol. Eng. **28:** 363–373, doi:10.1016/j.ecoleng.2006.06.010

Johansson, A. E., A. M. Gustavsson, M. G. Oquist, and B. H. Svensson. 2004. Methane emissions from a constructed wetland treating wastewater—seasonal and spatial distribution and dependence on edaphic factors. Water Res. **38:** 3960–3970, doi:10.1016/j.watres.2004.07.008

Kadlec, R. H., and R. L. Knight. 1996. Treatment wetlands. CRC Press.

———, C. C. Tanner, V. M. Hally, and M. M. Gibbs. 2005. Nitrogen spiralling in subsurface-flow constructed wetlands: Implications for treatment response. Ecol. Eng. **25:** 365–381, doi:10.1016/j.ecoleng.2005.06.009

Lund, L. J., A. J. Horne, and A. E. Williams. 1999. Estimating denitrification in a large constructed wetland using stable nitrogen isotope ratios. Ecol. Eng. **14:** 67–76, doi:10.1016/S0925-8574(99)00020-8

Matheson, F. E., M. L. Nguyen, A. B. Cooper, T. P. Burt, and D. C. Bull. 2002. Fate of ^{15}N-nitrate in unplanted, planted and harvested riparian wetland soil microcosms. Ecol. Eng. **19:** 249–264, doi:10.1016/S0925-8574(02)00093-9

Reinhardt, M., B. Muller, R. Gachter, and B. Wehrli. 2006. Nitrogen removal in a small constructed wetland: An isotope mass balance approach. Environ. Sci. Technol. **40:** 3313–3319, doi:10.1021/es052393d

Ruckauf, U., J. Augustin, R. Russow, and W. Merbach. 2004. Nitrate removal from drained and reflooded fen soils affected by soil N transformation processes and plant uptake. Soil Biol. Biochem. **36:** 77–90.

Scott, J. T., R. D. Doyle, and C. T. Filstrup. 2005. Periphyton nutrient limitation and nitrogen fixation potential along a wetland nutrient-depletion gradient. Wetlands **25:** 439–448, doi:10.1672/18

———, M. J. McCarthy, W. S. Gardner, and R. D. Doyle. 2008. Denitrification, dissimilatory nitrate reduction to ammonium, and nitrogen fixation along a nitrate concentration gradient in a created freshwater wetland. Biogeochemistry **87:** 99–111, doi:10.1007/s10533-007-9171-6

Shrestha, J., J. J. Rich, J. G. Ehrenfeld, and P. R. Jaffe. 2009. Oxidation of ammonium to nitrite under iron-reducing conditions in wetland soils laboratory, field demonstrations, and push–pull rate determination. Soil Sci. **174:** 156–164, doi:10.1097/SS.0b013e3181988fbf

Sigman, D. M., M. A. Altabet, R. Michener, D. C. McCorkle, B. Fry, and R. M. Holmes. 1997. Natural abundance–level measurement of the nitrogen isotopic composition of oceanic nitrate: An adaptation of the ammonia diffusion method. Mar. Chem. **57:** 227–242, doi:10.1016/S0304-4203(97)00009-1

Tobias, C. R., M. Cieri, B. J. Peterson, L. A. Deegan, J. Vallino, and J. Hughes. 2003a. Processing watershed-derived nitrogen in a well-flushed New England estuary. Limnol. and Oceanogr. **48:** 1766–1778.

———, A. Giblin, J. McClelland, J. Tucker, and B. Peterson. 2003b. Sediment DIN fluxes and preferential recycling of benthic microalgal nitrogen in a shallow macrotidal estuary. Mar. Ecol. Prog. Ser. **257:** 25–36, doi:10.3354/meps257025

———, S. A. Macko, I. C. Anderson, E. A. Canuel, and J. W. Harvey. 2001. Tracking the fate of a high concentration groundwater nitrate plume through a fringing marsh: A combined groundwater tracer and in situ isotope enrichment study. Limnol. Oceanogr. **46:** 1977–1989.

Vymazal, J. 2007. Removal of nutrients in various types of constructed wetlands. Sci. Total Environ. **380:** 48–65, doi:10.1016/j.scitotenv.2006.09.014

Associate editor: H. Maurice Valett

Received: 20 July 2009
Accepted: 25 November 2009
Amended: 19 January 2010